AAS-22-154

REDUCING JITTER DURING LARGE SLEWS USING MULTIFUNCTIONAL STRUCTURES FOR ATTITUDE CONTROL VIA TORQUE ANALYSIS

Vedant[*], James T. Allison[*†]

Multifunctional Structures for Attitude Control (MSAC) comprise a class of new attitude control systems that utilizes intelligent flexible deployable panels as attitude control actuators. Spacecraft attitude is modified via a repeated cycle of deformations achieved using embedded distributed strain actuators. Previously, MSAC has demonstrated the ability to rotate about a given axis for arbitrarily-large angles using non-holonomic control trajectories. Large attitude slews are achieved by oscillating the panels about two different axes, thereby modifying the mass moment of inertia between different phases of motion. Most control trajectories developed thus far have been based on dynamical models developed using conservation of angular momentum. In this article, the MSAC system model is developed using a torque interaction model, which is then used to design control trajectories that expand system operational envelopes and the pointing stability during slews. This paper concludes with simulation-based validation of the mechanical and control design of the MSAC system that improves system performance by reducing the vibrations introduced during attitude slews by almost 40 dB and increases the operational frequencies to beyond the first harmonic of the deployable panel.

INTRODUCTION

This paper details the improvements to the capabilities of a new attitude control system called Multifunctional Structure for Attitude Control (MSAC). MSAC utilizes flexible deployable panels with embedded strain actuators to oscillate the compliant panels, and utilize the reaction forces to provide attitude control. MSAC is an extension to the Strain Actuated Solar Arrays (SASA) attitude control system (ACS), which provides active jitter noise cancellation and small-angle attitude slews.[1] SASA has been designed to enable fine pointing accuracy/stability (up to sub-milli-arc-second level) for a wide variety of future spacecraft, enabling new science. Several studies have explored the system design,[2,3] system scaling[3] and optimal control co-design (CCD) of SASA.[4] The preliminary development of SASA was in collaboration with NASA Jet Propulsion Laboratory. Currently, SASA has been developed to a Technology Readiness Level of 6, in collaboration with CUA* supported by a NASA SBIR fund † in coordination with NASA Ames.

Although SASA is capable of fine pointing and stability, the system still relies on conventional ACS, such as Reaction Wheel Assemblies (RWAs) and Control Moment Gyroscopes (CMGs) for

*Department of Aerospace Engineering, University of Illinois at Urbana-Champaign, 104 S. Wright St., Urbana, IL 61801
†Department of Industrial and Enterprise Engineering, University of Illinois at Urbana-Champaign, 104 S. Mathews Ave., Urbana, IL 61801

*https://www.cuaerospace.com/

†https://sbir.nasa.gov/SBIR/abstracts/17/sbir/phase1/SBIR-17-1-S3.04-8406.html

M. Sandnas, D. B. Spencer (eds.), *Proceedings of the 44th Annual American Astronautical Society Guidance, Navigation, and Control Conference, 2022*, Advances in the Astronautical Sciences 179, https://doi.org/10.1007/978-3-031-51928-4_79

large attitude slews. MSAC augments SASA's capabilities and is capable of performing large attitude slews in addition to active jitter cancellation. Both SASA and MSAC eliminate a key failure mode (due to sliding friction, present in other momentum-exchange ACS technologies), through the use of a compliant distributed actuator design.[5] Some previous designs have utilized control schemes that are similar to MSAC,[6] but do not utilize multifunctional panels or the system compliance to provide the same amount of mass and volume savings, and still involve sliding contacts. The new capabilities of MSAC are enabled by modifications to the mechanical and control design of the SASA system. A summary of both the SASA and MSAC system, their comparisons to conventional ACS, and their applications to various missions types were presented in Ref.[7]

The extended capabilities of MSAC have been discovered and developed, using a lumped model for the actuators and the conservation of angular momentum. The developed lumped design does not eliminate the sliding mode of failure inherent to CMGs (control moment gyroscopes) and RWAs (reaction wheel assemblies), but provides a convenient framework for studying the system dynamics and estimating performance metrics.[8] Other previous studies have also explored the development of Pseudo Rigid Body Dynamics Models (PRBDMs), which allow approximating the compliant response using lumped degrees of freedom (DOFs), support analysis using simplified models, and aid design of complex systems.[9]

The MSAC model has been validated using FEA and Multi-body simulation studies.[8] A low-fidelity lumped prototype of MSAC has been validated using a low-cost one DOF roller-bearing based Hardware-in-the-loop (HIL) testbed.[10] This test puts the MSAC technology at a Technology Readiness Level (TRL) of 3. Other studies also explored the design of electronics with the mechanical systems to significantly increase the energy efficiency of the system, by leveraging mechanical and electrical resonances.[11] The same study[11] also introduced a different system architecture that does not rely on deployable panels to provide attitude control capabilities, called Cilia-MSAC. Cilia-MSAC enables the benefits of the MSAC concept to spacecraft that do not have large deployables or where the panels cannot be modified due to other requirements.

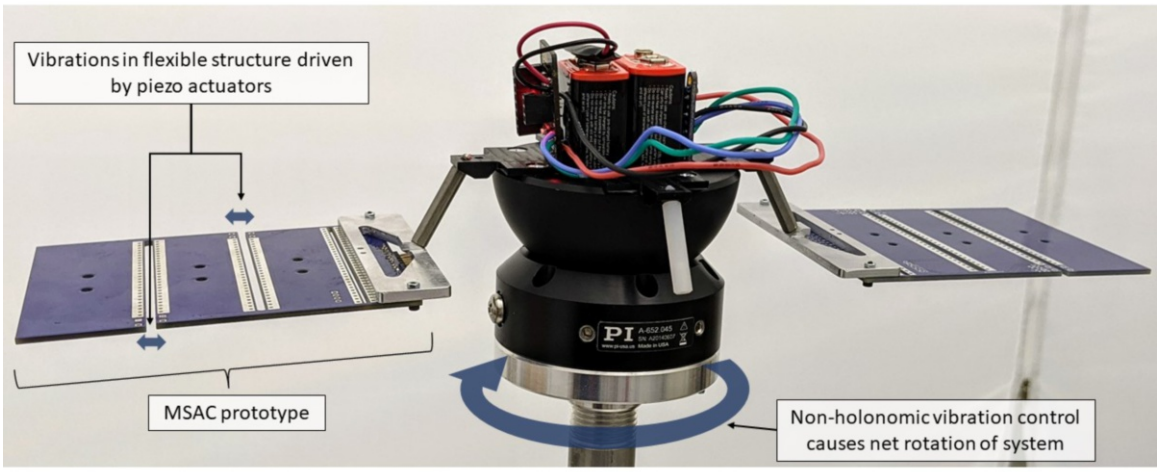

Figure 1: MSAC prototype (blue) on the spherical air-bearing based hardware test-bed used to confirm and validate the MSAC concept.

A high fidelity hardware-in-the-loop test was performed to validate a TRL 4 prototype on a spherical air-bearing test-bed. This setup can be seen in Fig.1. The prototype was sized for a CubeSat

deployable panel and demonstrated a peak slew rate of 0.2 rad/sec. The prototype was also tested and analyzed for fatigue effects and over a 24hr cumulative test span showed no evidence of fatigue failure onset.

MSAC and Cilia-MSAC have been filled for a provisional US patent through the University of Illinois. The US provisional patent for the core MSAC technology has been converted into an international filling through the Patent Cooperation Treaty. Subsequently, the technology has been patented non-provisionally as of December 2021.

Although MSAC eliminates the need for CMGs and RWAs for an ACS, the control trajectories developed thus far introduce significant vibrational disturbances during large slews. These disturbances limit pointing accuracy/stability when large slews are being executed, but when they are not, MSAC with existing control strategies is capable of ultra-fine pointing. The presence of vibration transmitted to the spacecraft bus during large slews has been identified by multiple stakeholders as an undesirable characteristic. This article presents a new strategy for mitigating MSAC vibration during large slews, which is facilitated by a new analytical approach.

In this study, a new dynamical model is developed using an interaction force model. This allows the development of strategic coupling mechanisms to the satellite bus. The design of these coupling mechanisms can act as a low-pass filter for the torques generated by MSAC, thereby significantly reducing the vibration experienced by the spacecraft during large slews. The new mathematical model also made possible the discovery of new control trajectories that can actively damp the vibrational noise generated by individual actuators, reducing the reliance on passive dynamics and expanding the operational bandwidth of the system.

The remainder of this article is composed of four main parts. The following section details the motivation for the development of a new model and the expected benefits. Next, the development of the mathematical models based on interaction torques is presented. The subsequent section details the development of passive system dynamics using the torque interaction models to reduce the MSAC mechanical vibrational noise transmitted to the spacecraft bus. Associated simulation results are also presented. Finally, we present the development of new control trajectories that further reduce vibrational noise, and support the expansion of MSAC operational frequencies.

MOTIVATION

The primary motivation for this study originated from the need to reduce mechanical noise transmitted to the spacecraft bus during large-slew MSAC operation. Having the capability of performing low jitter slews is desirable for observing/tracking objects that are not stationary with respect to inertial space. Most MSAC results communicated thus far have included a low-pass filtered estimate of the attitude of the spacecraft, which shows the secular (dc-component) of the attitude maneuver (for example, Refs.[8, 10]). Filtered estimates were obtained by applying a low-pass filter (such as a windowed moving average) to the attitude signal.

The post-processing filter applied in previous studies inspired a new strategy to reduce transmitted vibration. More specifically, instead of applying a filter in measurement, could a torque filter be realized in the MSAC embodiment? It is well known that in the electrical domain a low pass filter consists of a resistor-capacitor (RC) on the output of a signal. With the theory of bond graph modeling to aid description of analogous systems across different physics domains,[12] a similar result can be achieved in the mechanical domain with a spring-damper system.

MSAC development so far has been performed based on principles of conservation of angular

momentum. This analytical perspective has been useful for numerous studies, but does not provide direct insight into the design of spring-damper elements for vibration isolation. A new analytical perspective is needed. A section-wise torque interaction model was developed to support tracking of pertinent states (torques produced by each panel/panel section) in time, and the observation of the effects of including spring-damper components at various locations.

MODEL DEVELOPMENT

In previous studies, MSAC was analyzed by approximating the compliant distributed actuators by lumped Degrees of Freedom (DOFs) joints and conservation of angular momentum to develop a simplified system model, which was used to derive preliminary system performance estimates.[8] Using this earlier momentum-based model, it was discovered that actuating the MSAC system close to the primary harmonic of the deployable panel provided the most slew efficiency. The HIL demonstration was also at an actuation frequency close to the primary harmonic of the deployable panel. The selection of this actuation frequency also allows the production of the largest slew rates with a given actuator and mechanical design.

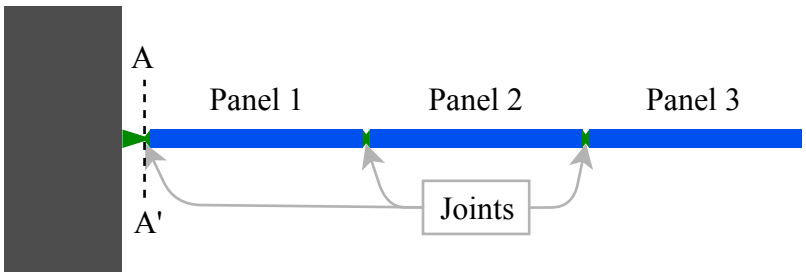

Figure 2: MSAC panel (right of the line AA' attached to a spacecraft(grey), each panel section (blue) is labeled, along with a 2-DOF joint (green) between panel sections).

Here, the MSAC model is analyzed from a torque interaction perspective. This model is developed such that MSAC performance can be evaluated independently of spacecraft bus properties. This decoupling of dynamics facilitates the rapid development of mechanically sophisticated MSAC designs by decoupling the multifunctional panel from the spacecraft. In Fig. 2, the MSAC system is shown with the satellite body and a deployable panel, separated by the imaginary line AA'. The current model development focuses on the deployable panels, to the right of line AA'. The panel shows three rigid panel sections (blue) with three joints (green), each having two DOFs: revolution, and extension.

To further simplify the model, only the first rigid section of the deployable panel is considered with a 2-DOF joint. The first section of the deployable panel is illustrated in Fig. 3. The panel section is assumed to execute one of two unique control trajectories that enable attitude slews. In Fig. 3, the panel is blue when in contraction, and red when in extension; this is a longitudinal vibration enabled by the strain actuators. The transverse oscillations are responsible for bending the panel back and forth. The central circular arrow indicates the sequence of motions performed using the panel to perform an anti-clockwise slew. To perform a clockwise slew, the direction of the transverse oscillation must be reversed.

To develop the mathematical model, the control trajectory is split into the four phases shown in Fig. 3, performed at an actuation frequency close to the natural frequency for the associated motion.

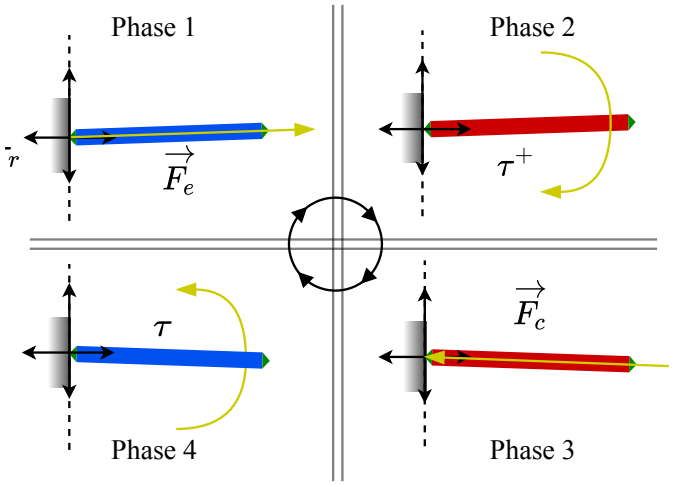

Figure 3: Visualization of the periodic non-holonomic control trajectory for a panel section which enables production of a average reaction torque τ_r during one cycle. All force and torque vectors are shown (yellow); the attitude slew is a rotation about an axis going into the plane of the page.

The motions of the panels are constrained to an extended length of l_e and a bending angle of $\pm\theta$ about the rest position.

During Phases 1 and 3, the panel produces forces that extend and contract the panel, respectively. The reaction forces will translate the spacecraft, but most deployable panes are symmetric about the spacecraft, and hence the reaction forces produced by the pair are canceled. The main contribution of this phase of motion is to modify the mass moment of inertia of the panel. The difference in the Moment of Inertia (MOI) is shown in Eqs. (1) and (2):

$$I_p = \frac{1}{12} m_p (l_p^2 + w_p^2), \tag{1}$$

$$I_e = \frac{1}{12} m_p (l_e^2 + w_p^2), \tag{2}$$

where m_p is the panel section mass, w_p is the panel section width, l_p is the panel section length at rest, and l_e is the panel length after extension. The panel MOI is calculated by assuming the panel is a uniform-density rectangular prism.

Phases 2 and 4 are utilized to bend the panels back and forth to apply torques to produce the attitude slew. The panels are rotated from θ to $-\theta$ in Phase 2, and back in Phase 4. The net torque applied during these motions is the same τ, but due to the difference in the MOI, the time required for these motions is different. This difference is quantified in Eqs. (3) and (4):

$$t = \sqrt{\frac{4\theta I_p}{\tau}}, \tag{3}$$

$$t^+ = \sqrt{\frac{4\theta I_e}{\tau}}, \tag{4}$$

where t^+ refers to the increased time required when the panel is extended.

The difference in time t and t^+ in effect, produces different angular impulses for the two different phases. An estimate of the angular impulse produced for phases of the control trajectory is presented

in Eqs. (5) - (8):

$$A_{\mathrm{P1}} = 0 \tag{5}$$
$$A_{\mathrm{P3}} = 0 \tag{6}$$
$$A_{\mathrm{P2}} = -t\tau \tag{7}$$
$$A_{\mathrm{P4}} = t^{+}\tau, \tag{8}$$

where A_{Pi} is the angular impulse produced for the i^{th} phase.

The effective reaction torque produced by the panels is quantified in Eq. (10) upon simplification:

$$\tau_r = \frac{-(A_{\mathrm{P2}} + A_{\mathrm{P4}})}{T} \tag{9}$$
$$= \frac{\tau(t - t^{+})}{t + t^{+} + t_e + t_c}, \tag{10}$$

where T is the time period of the periodic control trajectory, and t_e and t_c are the times required for panel extension and contraction, respectively.

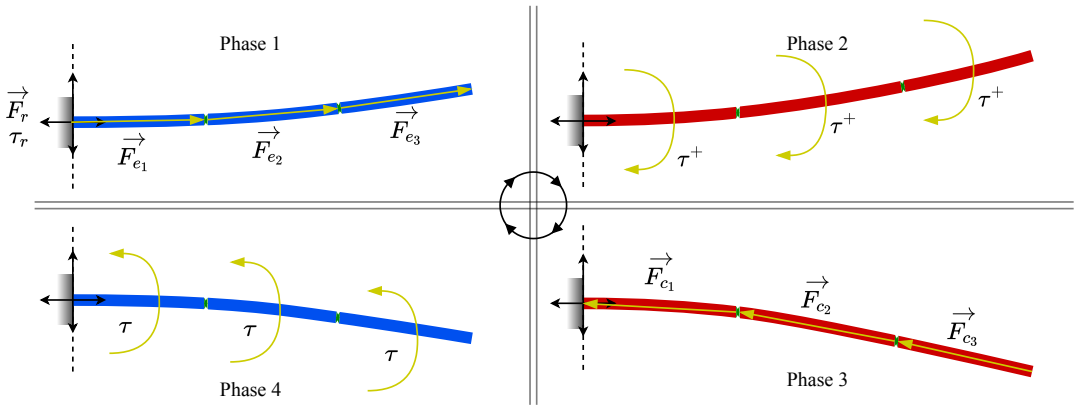

Figure 4: Visualization of the periodic non-holonomic control trajectory for a full MSAC panel, which enables the production of an average torque $n\tau_r$ during one cycle, where n is the number of panel sections. All force and torque vectors are shown (yellow), and the attitude slew is a rotation about an axis going into the plane of the page.

With the force and torque estimation for a pair of panel sections on the spacecraft derived, the forces and torques due to all deployable panel sections can be estimated for the control trajectories shown in Fig. 4. The net force applied can be kept to a minimum by using symmetrical deployable panels that cancel the translational forces produced. The torques will scale linearly with the number of panel sections added, assuming the changes to the panel inertia are accounted for and small-angle approximation is considered, following the law of superposition. The average reaction torque produced by an MSAC panel consisting of k-panel sections is given by Eq. (11).

$$\tau_r = \frac{k\tau(t - t^{+})}{t + t^{+} + t_e + t_c} \tag{11}$$

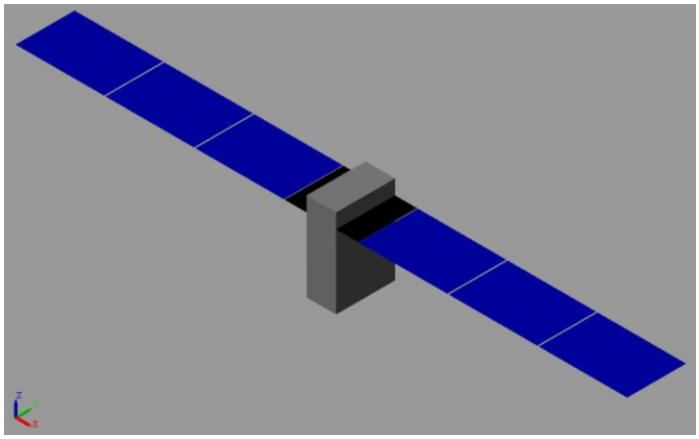

Figure 5: 6U-CubeSat with a pair of three-section foldable deployables, with three panel sections on each side. The mechanical coupling between MSAC and the spaccraft is shown as the black panel section.

The derivation of a force-torque estimate also shows that the MSAC panels produce both τ and $-\tau$ for two of the four phases of the control trajectory, with no torque produced during other phases. To reduce the variation of the torque produced on the spacecraft, the MSAC panel can be attached to a mechanism designed to average the torques (i.e., a mechanical low pass filter), as a strategy to reduce the vibrational jitter. This low pass filter in a mechanical system is achieved by inserting a spring-mass-damper in the sequence of force/torque transmission elements. A low pass filter can be achieved by changing the passive dynamics of the root joint (left most joint in Fig. 2) to transmit only the low-frequency components of the panel torque. Practically, this can be achieved by designing the root actuator with an appropriate spring stiffness and damping rate.

RESULTS AND DISCUSSION

A Simulink model was created that mimics the inertial properties of an MSAC system for a 6U-CubeSat with multifunctional deployable solar panels, as seen in Fig. 5. The 6U-CubeSat model is assumed to have deployable solar panels with three-panel sections on either side. These MSAC capable panels (blue) are assumed to have distributed actuators that provide MSAC capability. The deployment mechanism of the solar panel (black) also serves as the means of coupling MSAC with the spacecraft, whose passive dynamics are tailored to significantly reduce the vibration transmitted from the MSAC panels to the spacecraft bus. Specifically, the spring and damper coefficients for the joint between the black and first blue panel section was changed to reduce jitter. The jitter reduction for other panel section arrangements can be performed in a similar manner.

To ensure simulation accuracy the relative tolerance and absolute tolerance were set to 10^{-8} instead of the default solver values of 10^{-6}. All simulations were performed for a time horizon of 10 seconds to ensure that the MSAC system attains periodic steady-state operation. The satellite is slewing about the positive y-axis of the world frame shown in Fig. 5.

Jitter reduction through passive damping

Figure 6 shows the frequency response of the attitude slew angle of the CubeSat bus, from the angle axis representation. The waveforms show the fast Fourier transform (FFT) response for two

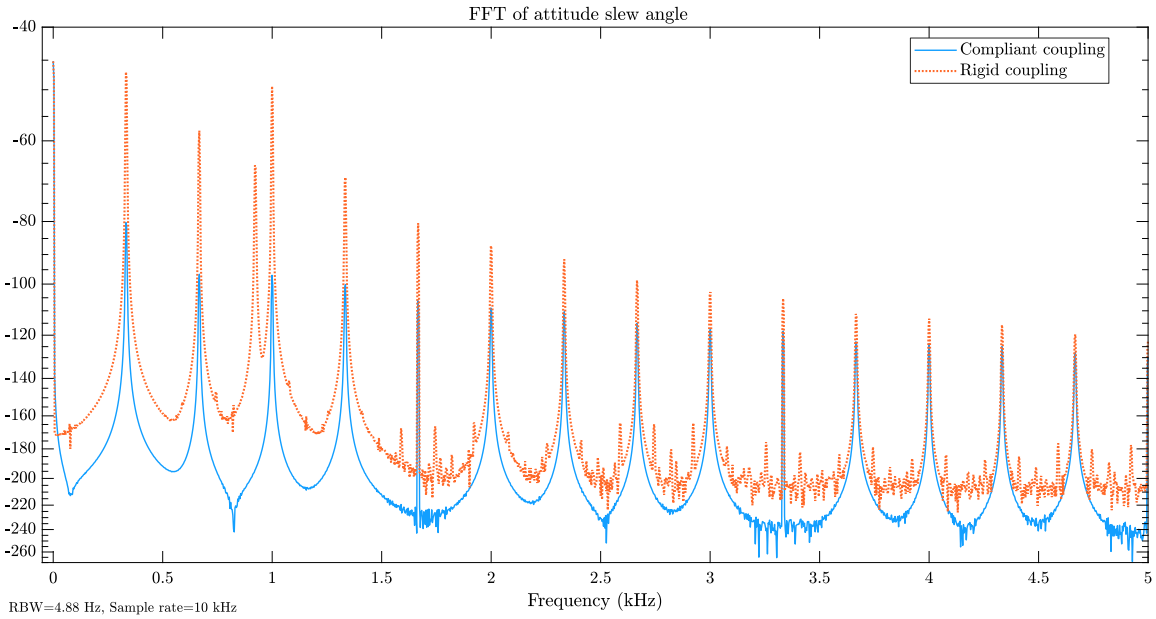

Figure 6: Frequency response of the attitude slew angle of the spacecraft. The dashed line shows the response for an undamped/rigid coupled MSAC system, whereas the solid line shows an MSAC system with a tuned compliant root joint. The passive dynamics of the root joint isolate the mechanical jitter introduced by MSAC during a slew from the spacecraft.

different system coupling, one where the MSAC panels are connected to the 6U-CubeSat using a stiff/rigid coupling (i.e spring stiffness is ∞), while the second case shows the response of using a compliant MSAC panel coupling with a revolute joint of spring stiffness is 16 N-m/rad.

The signal is sampled at 10kHz, and hence the FFT x-axis has a range of 0 to 5kHz. The peak at the origin is the dc component of the slew, also known as the average attitude changed. The peaks beyond origin are the harmonic modes of the mechanical noise experienced by the system. The left plot is that of the undamped MSAC system, whereas the response shown on the right corresponds to the tuned passive system. The difference in the magnitude of vibrational noise amplitude in the primary vibrational mode is approximately 40 dB, with significant improvements for higher resonance modes. The highest peak (dc-component) is unaltered in height, which indicates that the system performance has not been diminished by the modification of the base joint to have a different spring stiffness and damper characteristic.

Jitter reduction through active damping

The models based on torque interactions allow for the development of more advanced control trajectories. One such control trajectory is illustrated in Fig. 7. Here, each subsequent panel section is 180° out of phase with the other. Therefore, every alternate panel section is two phases apart in the control trajectory. Using this fact and the principle of superposition, an estimate of the angular impulse produced for Bending 1 and Bending 2 sections of the control trajectory is presented in

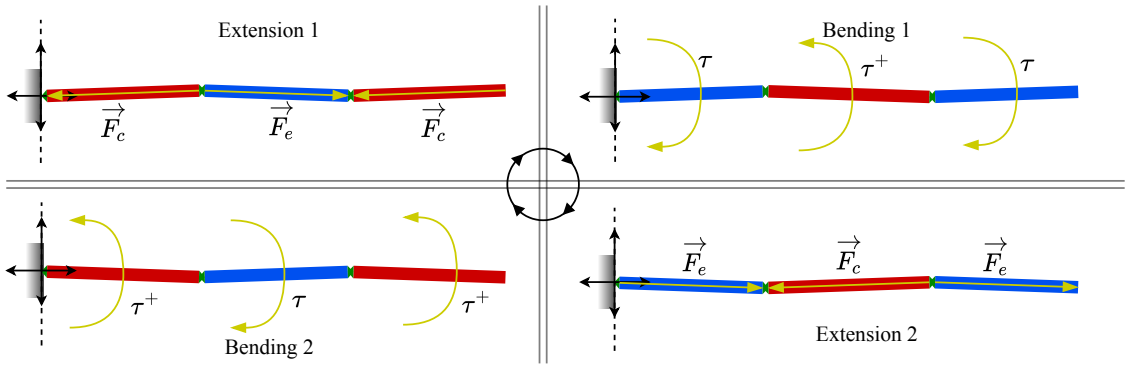

Figure 7: Visualization of a periodic non-holonomic control trajectory for a full MSAC panel, which reduces the jitter produced and expands the operational bandwidth of MSAC. All force and torque vectors are shown (yellow), the attitude slew is a rotation about an axis going into the plane of the page.

Eq. (12) and Eq. (13), respectively:

$$A_1 = (mt^+ - nt)\tau \tag{12}$$
$$A_2 = (nt^+ - mt)\tau, \tag{13}$$

where n is the number of panel sections in Phase 2 of the control trajectory, and m is the number of panel sections in Phase 4.

This trajectory will actively cancel the effective torque noise produced by each section, reducing the reliance on a symmetric distribution of panels for force cancellations, and produce a more even torque throughout the control trajectory. The reduced torque ripple reduces the need for passive dynamics tuning for the reduction of the vibrational noise. The effective average reaction torque produced due to this trajectory is given by Eq. (16) upon simplification:

$$\tau_r = \frac{-(A_1 + A_2)}{T} \tag{14}$$
$$= \frac{-((mt^+ - nt)\tau + (nt^+ - mt)\tau)}{t + t^+ + t_e + t_c} \tag{15}$$
$$= \frac{(n+m)(t - t^+)\tau}{t + t^+ + t_e + t_c}. \tag{16}$$

Additionally, since the system response time and bandwidth are dictated by the resonance frequency, developing control trajectories for each panel section instead of for the whole panel expands the bandwidth of operation. The higher bandwidth is because each panel section is smaller than the whole panel and hence has a significantly higher bandwidth natural frequency, due to the lower effective inertia.

The frequency response of the torque experienced by the spacecraft can be seen in Fig. 8. The figure demonstrates all four cases:

1. Rigid Coupling: No passive or active considerations have been made in the design of the MSAC system. This system design yields the highest level of jitter introduced into the spacecraft during slews.

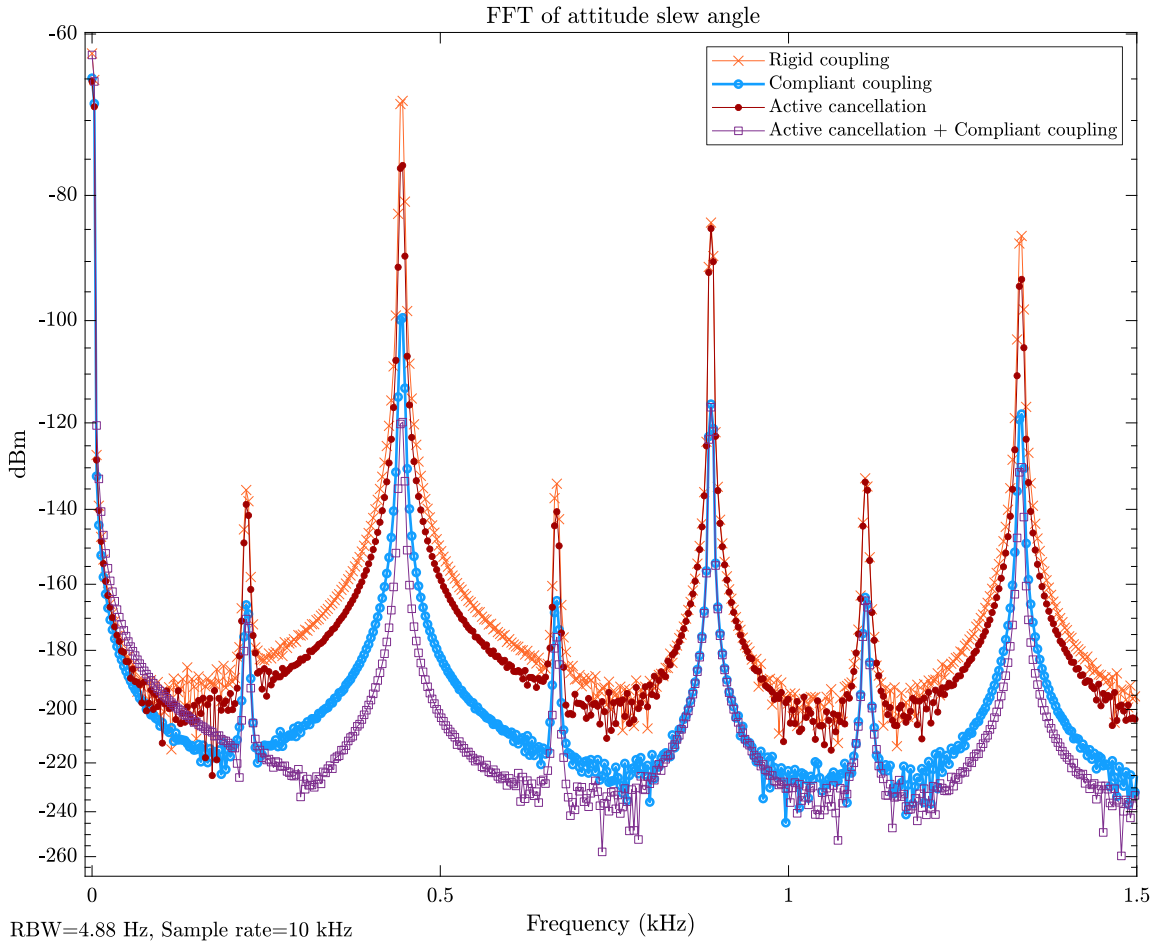

Figure 8: Frequency response of the attitude slew angle of the spacecraft. The responses of four system design cases are shown: rigid coupling, compliant coupling, active cancellation with rigid coupling, and active cancellation with complaint coupling. The first two cases are identical to those in Fig. 6.

2. Compliant Coupling: The passive dynamics of the component that couples MSAC with the spacecraft is tuned to isolate the bus from high-frequency components of the MSAC panel vibrations, thereby reducing the jitter experienced by the spacecraft during slewing. The reduction of jitter/ripple in the torque generated by MSAC comes at the cost of reduced control authority at high frequencies due to the passive low-pass filter coupling MSAC to the spacecraft.

3. Active Cancellation: The control trajectory of each deployable panel, shown in Fig. 5, is implemented with a 120° deg phase offset with respect to its neighbors. The result of this can be seen in Fig. 8. Although the harmonics are reduced, the noise reduction is not close to the passive tuned case. This reduced performance comes at the benefit of maintaining the control authority of the MSAC system over a wider bandwidth. The reduction in the amplitude of the harmonics can be further reduced by matching more panel sections which would result in a reduction of ripples in the torques produced by the MSAC system. The jitter at higher

frequencies are more difficult to actively cancel due to the timing requirements for phase cancellation, therefore the higher harmonics are not attenuated as much.

4. Active Cancellation and Compliant Coupling: The utilization of both passive damping and active cancellation provide the best performance of the system. This is a consequence of optimizing the mechanical and control system design iteratively, also known as iterated sequential Control Co-Design (CCD) optimization.[13] The active cancellation reduces the reliance on a low pass filter, allowing the incorporation of a less agressive filter that supports a larger operational bandwidth for MSAC. Passive compliance reduces the high-frequency jitter/ripple that is challenging to cancel using active control.

CONCLUSION AND FUTURE WORK

In this study, a new mathematical model for Multifunctional Structures for Attitude Control (MSAC) was developed, utilizing Newtonian reaction force models and Pseudo Rigid Body Models.[9] Compared to previous models for MSAC,[8] this model provides new utility for exploring transient behavior. Using the new model, insights were derived, and the system performance was expanded and improved. Feasible changes to the passive dynamics of the joint design have been shown to increase pointing stability during attitude slews. Other new control trajectories have also been formulated which reduce the reliance on the passive dynamics and reduce the vibrational noise produced by MSAC while increasing the operating frequency range of the system.

In future studies, control co-design[13,14] optimization will be used to explore the best passive dynamics for a particular system design. The impact of the tailored passive dynamics to suppress the jitter produced by MSAC during slewing versus active jitter damping capabilities of MSAC against external noise sources will be explored. The active damping trajectories synthesized in the final parts of the paper will be validated using simulation studies to also explore the mechanical design topologies which improve performance and robustness to system failure modes.

ACKNOWLEDGMENTS

This material is based upon work partially supported by the National Science Foundation under Grant No. CMMI-1653118.

REFERENCES

[1] O. S. Alvarez-Salazar, J. B. Aldrich, J. T. Allison, and S.-J. Chung, "Strain Actuated Solar Arrays for Precision Pointing of Spacecraft," 2016 AAS Guidance, Navigation, and Control Conference, Breckenridge, CO, USA, Feb. 2016.

[2] C. M. Chilan, D. R. Herber, Y. K. Nakka, S.-J. Chung, J. T. Allison, J. B. Aldrich, and O. S. Alvarez-Salazar, "Co-Design of Strain-Actuated Solar Arrays for Spacecraft Precision Pointing and Jitter Reduction," AIAA Journal, Vol. 55, Sept. 2017, pp. 3180–3195, 10.2514/1.J055748.

[3] D. R. Herber, J. W. McDonald, O. S. Alvarez-Salazar, G. Krishnan, and J. T. Allison, "Reducing spacecraft jitter during satellite reorientation maneuvers via solar array dynamics," 15th AIAA/ISSMO Multidisciplinary Analysis and Optimization Conference, 2014, p. 3278.

[4] Y. K. Nakka, S.-J. Chung, J. T. Allison, J. B. Aldrich, and O. S. Alvarez-Salazar, "Nonlinear Attitude Control of a Spacecraft with Distributed Actuation of Solar Arrays," Journal of Guidance, Control, and Dynamics, Vol. 42, No. 3, 2019, pp. 458–475.

[5] D. F. Machekposhti, N. Tolou, and J. Herder, "A review on compliant joints and rigid-body constant velocity universal joints toward the design of compliant homokinetic couplings," Journal of Mechanical Design, Vol. 137, No. 3, 2015, p. 032301.

[6] V. Coverstone-Carroll and N. Wilkey, "Optimal control of a satellite-robot system using direct collocation with non-linear programming," Acta Astronautica, Vol. 36, No. 3, 1995, pp. 149–162.

[7] Vedant, A. Ghosh, O. S. Alvarez-Salazar, and J. T. Allison, "Impact of Strain-Actuated Attitude Control Systems for Variant Mission Classes," 70th International Astronautical Congress, No. C1.5.2, Washington D.C., United States, Oct. 2019.

[8] Vedant and J. T. Allison, "Multifunctional Structures for Attitude Control," Vol. ASME 2019 Conference on Smart Materials, Adaptive Structures and Intelligent Systems of Smart Materials, Adaptive Structures and Intelligent Systems, 09 2019. V001T03A005, 10.1115/SMASIS2019-5565.

[9] Vedant and J. T. Allison, "Pseudo-Rigid-Body Dynamic Models for design of compliant members," Journal of Mechanical Design, 12 2019, pp. 1–22, 10.1115/1.4045602.

[10] Vedant, A. E. Patterson, and J. T. Allison, "Multifunctional Structures for Spacecraft Attitude Control," 2020 AAS Guidance & Control Conference, 2020.

[11] Vedant and J. T. Allison, "Impact of including electronics design on design of intelligent structures: Applications to Multifunctional Structures for Attitude Control (MSAC)," Smart Materials, Adaptive Structures and Intelligent Systems, 09 2020. Conditionally accepted to ASME 2020 Conference on Smart Materials, Adaptive Structures and Intelligent Systems.

[12] W. Borutzky, Bond graph modelling of engineering systems, Vol. 103. Springer, 2011.

[13] J. T. Allison and D. R. Herber, "Special Section on Multidisciplinary Design Optimization: Multidisciplinary Design Optimization of Dynamic Engineering Systems," AIAA journal, Vol. 52, No. 4, 2014, pp. 691–710.

[14] J. T. Allison and D. R. Herber, "Multidisciplinary Design Optimization of Dynamic Engineering Systems," AIAA Journal, Vol. 52, Apr. 2014, pp. 691–710, 10.2514/1.J052182.